Theor Chem Acc (2004) 112: 290–297
DOI 10.1007/s00214-004-0579-y

Theoretical
Chemistry Accounts

Regular article

Acid-catalysed oxidative ring-opening of epoxide by DMSO. Theoretical investigation of the effect of acid catalysts and substituents

Sylvain Antoniotti, Serge Antonczak, Jérôme Golebiowski

Laboratoire Arômes Synthèses Interactions, Faculté des Sciences, Université de Nice Sophia-Antipolis,
Parc Valrose, 06108, Nice Cedex 2, France

Received: 25 July 2003 / Accepted: 18 December 2003 / Published online: 29 April 2004

Abstract. DFT studies have been carried out in order to investigate the reaction mechanism of a series of acid-catalysed oxidative ring-opening of epoxides in DMSO. The role of the acid catalyst during the oxidation of ethylene oxide has been investigated by employing three acids, namely H_3O^+, Li^+, and Mg^{2+}. Effects of substituents on the epoxide have been investigated by including butene oxide and cyclopentene oxide as the reacting species. Stationary points have been obtained at the B3LYP/6–31 + + G(d,p) level of theory and the reaction barriers have been evaluated through free-energy calculations. This is the first mechanistic elucidation for such a process, involving oxidation of the epoxide ring by DMSO. The mechanism proceeds in two steps, namely a ring-opening step followed by an intramolecular proton transfer which leads to an α-hydroxyketol. The results show that the second step is the energetically less favourable, a feature consistent with the harsh experimental conditions needed to obtain such products. The role of the acid catalyst is discussed and we show that use of H_3O^+ or Mg^{2+} as an activator leads to similar results concerning the reaction energetics.

Keywords: Density functional theory – Epoxide – Ring-opening Lewis acid-catalyst – Reaction mechanisms

Introduction

Epoxides are known to be important intermediates in organic synthesis, as they can potentially be converted into a large number of functional groups and chiral products, by various ring-opening addition and isomerisation reactions [1–7].

Despite the large number of papers dealing with epoxide transformations, oxidation reactions have, up to now, received only limited interest. Such oxidative processes are made possible through the use of an oxygen donor within the system, together with different kinds of acid catalyst, such as $BF_3.Et_2O$ [8] and Me_3 SOTf [9], or Brönsted acids such as CF_3COOH and CF_3SO_3H [10, 11]. The use of dimethyl sulfoxide (DMSO) has been described as playing the role of solvent and oxidant in such reactions [12–14].

Oxidation processes based on the use of DMSO are involved in various syntheses [12, 13, 14]. Applied to epoxides, acid-catalysed DMSO-based oxidations can proceed either through C–C bond cleavage of the epoxide ring, and eventually lead to different kinds of product such as aldehydes and carboxylic acids [15], or without C–C bond cleavage and lead to α-functionalised ketones such as α-ketols [10] and α-diketones [16, 17]. The reaction mechanism of such epoxide oxidative ring-opening is still unknown. In this work, we explore the reaction pathways and especially the effect of the catalyst and substituents on the starting epoxide, by means of density functional calculations.

Method

Calculations were performed using the Gaussian98 suite of programs [18]. Geometries were optimised at the B3LYP level [19, 20]. The B3LYP functionals have allowed us to consider a large number of calculations that could not have been conducted at any higher level of theory. To assess the validity of a DFT-based approach we have conducted calculations at CCSD(T) level of theory. Table 1 presents the reaction free energies for the oxidative opening of ethylene oxide with both B3LYP and coupled cluster Hamiltonians, considering the two steps of the oxidative ring-opening process, as depicted in Scheme 1.

Proceedings of the 11th International Congress of Quantum Chemistry satellite meeting in honor of Jean-Louis Rivail

Correspondence to: Jérôme Golebiowski
e-mail: Jerome.golebiowski@unice.fr

Table 1. Ethylene oxide oxidative ring-opening reaction free energies (two steps) at B3LYP and CCSD(T) levels of theory, in kcal·mol^{-1}. See text for details

Level of theory/Basis set	First step	Second step
B3LYP/6–31 + + G(d,p)	−23.2	−30.7
CCSD(T)/6–31 + + G(d,p)	−24.8	−27.9

Since, to our knowledge, no accurate experimental value is available, CCSD(T) can be considered to give reference values for this reaction. The small difference between B3LYP and the much more time-consuming CCSD(T) results (respectively 6.5% and 9% for steps 1 and 2) confirms the possibility of using the B3LYP set of functionals in the rest of the studies.

The necessity of considering polarisation functions to properly describe sulfoxide-containing systems has been clearly discussed [21–23]. However, Cubbage et al. concluded that even a relatively modest basis set such as 6–31G(d,p) could give energetic results in an acceptable range [21]. We have, however, chosen to add diffuse functions to all atoms in our system, considering that proton exchange could occur in the oxidative process of the reaction.

Harmonic vibrational frequencies were obtained at the same level of calculations (B3LYP/6–31 + + G(d,p)) and were used to characterise energy minima (no imaginary frequency) and first-order saddle points (one imaginary frequency). Thermal corrections to Gibbs free energy results and zero point energy values were also obtained from the frequency calculations. Connection between the minima and the corresponding transition states have been checked by means of IRC calculations.

In order to analyse the role of electronic polarisation of ethylene oxide in the geometry of the complex with a metal cation, let us write the interaction energy between the epoxide and the cation charge as:

$$\left\langle \Psi^{pol} \middle| \hat{H}^0 + \hat{V}^q \middle| \Psi^{pol} \right\rangle - \left\langle \Psi^0 \middle| \hat{H}^0 \middle| \Psi^0 \right\rangle \quad (1)$$

where $\hat{H}^0$ is the epoxide Hamiltonian in a vacuum and $\hat{V}^q$ the coulomb potential created by the cation. $\left\langle \Psi^0 \middle| \hat{H}^0 \middle| \Psi^0 \right\rangle$ is the energy of the unpolarised epoxide and $\left\langle \Psi^{pol} \middle| \hat{H}^0 + \hat{V}^q \middle| \Psi^{pol} \right\rangle$ is the energy of the polarised epoxide in the presence of the cation charge. The electronic polarisation component is obtained from:

$$\left\langle \Psi^{pol} \middle| \hat{H}^0 + \hat{V}^q \middle| \Psi^{pol} \right\rangle - \left\langle \Psi^0 \middle| \hat{H}^0 + \hat{V}^q \middle| \Psi^0 \right\rangle \quad (2)$$

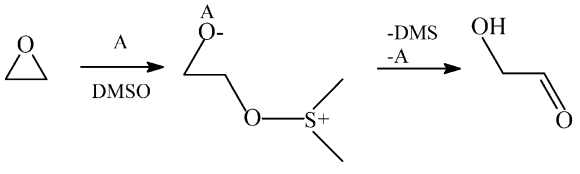

Scheme 1. Acid-catalysed oxidative ring-opening of epoxide by DMSO

Such energy decomposition should be useful in the analysis of the energy components between the cationic catalyst and the epoxide ring.

Results and discussion

Nucleophilic attack and epoxide opening by DMSO

From experimental studies of the Brönsted acid-catalysed oxidation of cyclohexene oxide and styrene oxide (**4** and **5**, respectively, in Scheme 2), it is known that activation of the epoxide by the acid catalyst results in nucleophilic ring-opening of this activated epoxide by DMSO. An α-hydroxyalkoxysulfonium ion is formed as an intermediate and has been isolated in its salt form with the corresponding counter-ion provided by the Brönsted acid [10]. This intermediate is the starting point for a second step during which an oxidation process occurs, leading to α-hydroxycarbonyl compounds.

Stationary points for such a transformation have been characterised using model epoxides and model catalysts. We have first chosen to consider the smallest epoxide, ethylene oxide (**1** in Scheme 2), which allows us to envisage various activation effects in reduced calculation times. In addition, in an effort to rationalise the effect of the 1,2-substituents on the epoxide, two other reactants have been investigated, butene oxide (both *cis* and *trans*-forms have been considered, further labelled $\mathbf{2}^{cis}$ and $\mathbf{2}^{trans}$) and cyclopentene oxide (**3**). The latter may provide information on the effect of strain and steric hindrance through such a reaction.

Moreover, to assess the effect of the catalyst, we have performed our calculations with three different acids, namely H_3O^+, the singly-charged Li^+ cation, and the doubly-charged Mg^{2+} cation. These three activating species have been introduced for the reaction involving ethylene oxide, whereas only H_3O^+ acid has been used for all the epoxides (**1**, $\mathbf{2}^{cis}$, $\mathbf{2}^{trans}$, and **3**).

For the sake of simplicity and minimising confusion, all the structures related to the nucleophilic attack of DMSO on the various epoxides are denoted as CPX1, TS1, and PD1 for the first step of ring-opening and TS2 and PD2 for the second step of the oxidative process. The nature of the catalyst and the epoxide will be specified when necessary. For butene oxide, unless specified otherwise, values in the figures, tables, and in the text all refer to *cis* configuration since only slight differences have been observed between the two isomers. A representation of the reaction path is given in Figs. 1a and 1b. Structures of the complexes, transition states,

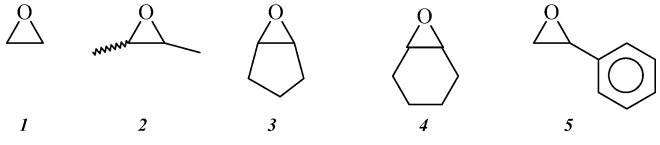

Scheme 2. Representation and labelling of the different epoxides discussed in the text

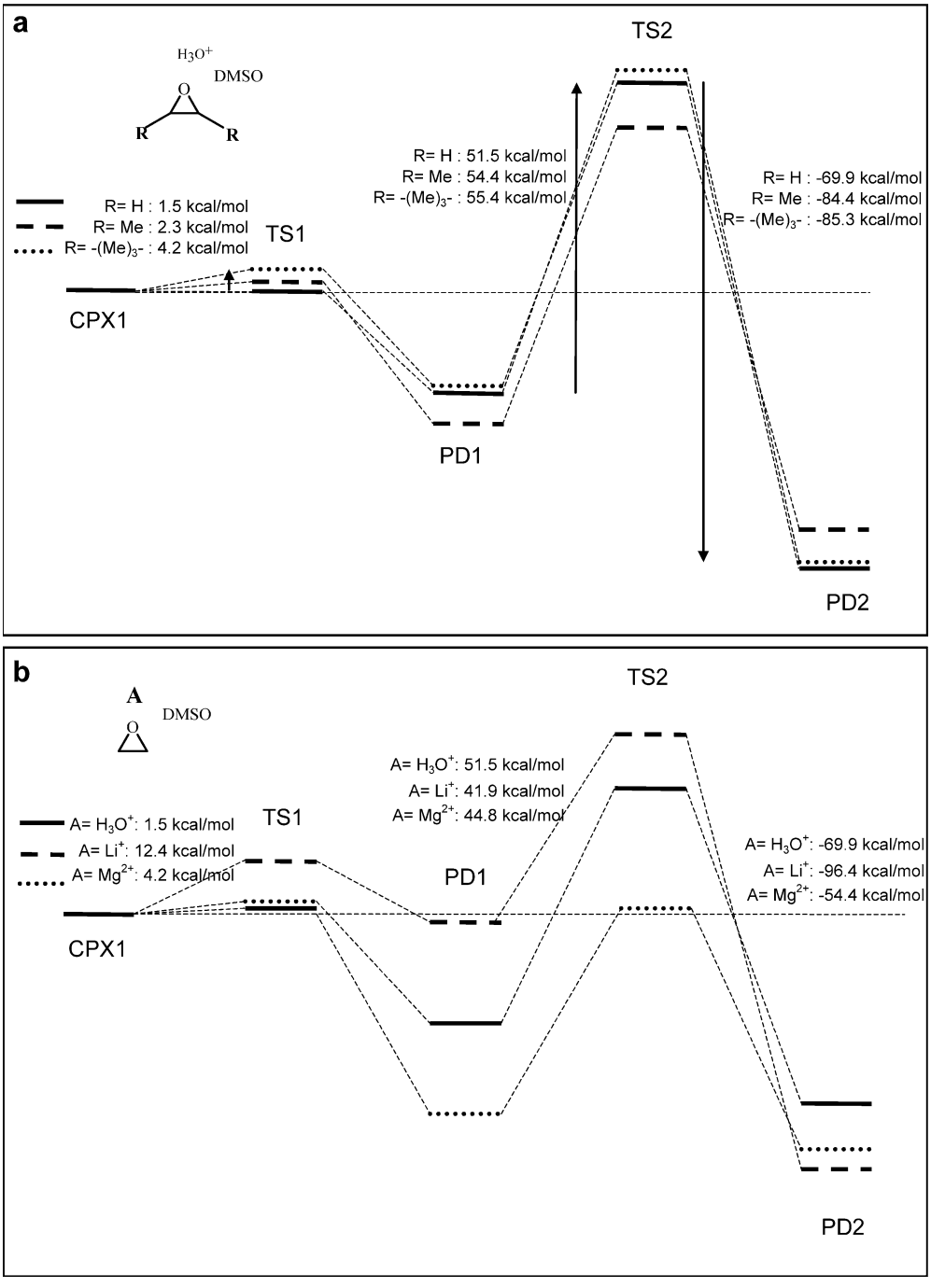

Fig. 1. (**a**) Reaction pathways for H_3O^+-catalysed oxidative ring-opening by DMSO with various epoxides. (**b**) Reaction pathways for the H_3O^+, Li^+, and Mg^{2+} acid-catalysed oxidative ring-opening by DMSO of ethylene oxide. Barrier heights and final product exothermicity are shown. Values for the simplest model **1**/H_3O^+ are given in both figures

and products are presented in Fig. 2, for comparison of the influence of the Lewis acid, and in Fig. 3 for analysis of the role of the 1,2 substituent.

The ring-opening process consists in an S_N2 attack of DMSO on one of the two carbon atoms of the activated epoxide. Prevalence of the S_N2 process with respect to the S_N1 process has been evaluated to be more than 40 kcal mol^{-1} for the ethylene oxide/H_3O^+ system. Therefore, the S_N1 process has not been investigated further on other systems, due to its large activation energy.

Also, theoretical investigation of epoxide ring-opening reaction without catalyst did not lead to stationary points similar to those found with a cationic catalyst, confirming the crucial role played by the cation throughout the reaction.

Structural evolution

Concerning the starting complex, CPX1, some discrepancies in the C–O bond lengths and in the DMSO/epoxide distances can be put forward depending on the activating species. The different behaviour of the Li^+ and Mg^{2+} Lewis acid metal centres and the Brönsted acid arises mainly from the difference in the charge of the catalyst and

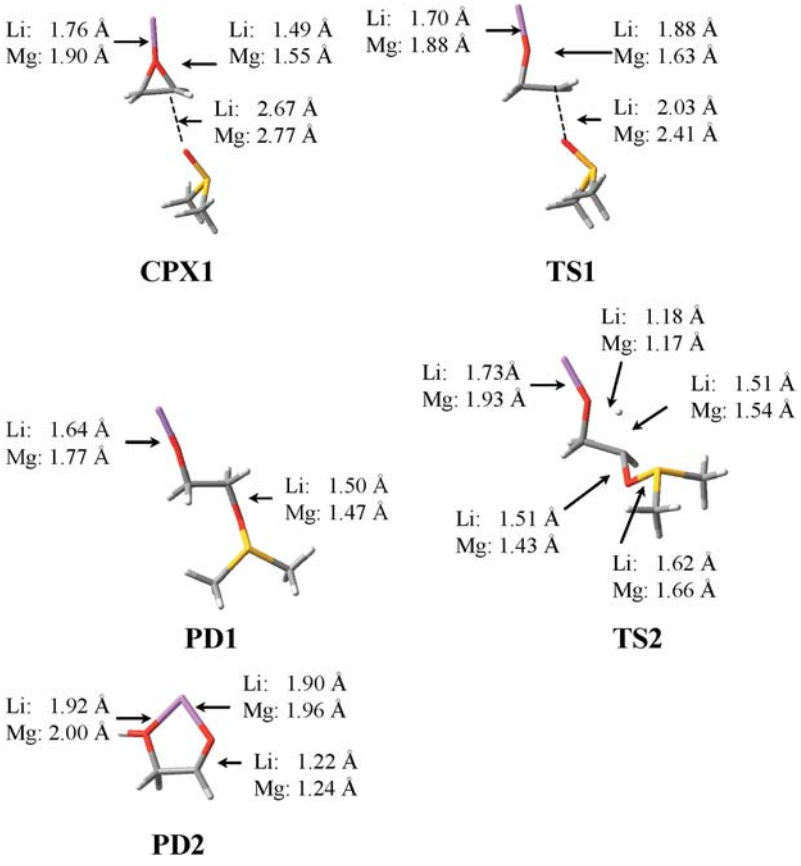

Fig. 2. Optimised structures with characteristic distances of the DMSO/epoxide/metal systems. PD2 DMS molecule is not shown

in the structural evolution of the complex within the reaction process. While H_3O^+ is able to transfer a proton to the oxygen atom of the epoxide, leading to the formation of a covalent O–H bond (dO–H≈1 Å), the Lewis acids, in contrast, can only act through an electrostatic interaction. With H_3O^+, the system can thus be considered as a formally charged protonated epoxide, solvated by a water molecule. These different effects lead, for example, to some interesting variations in the DMSO oxygen atom and the epoxide carbon atom distance. Indeed, d(C–O) is 2.51 Å, 2.67 Å, and 2.77 Å for H_3O^+, Li^+ and Mg^{2+} respectively. Concerning the activated C–O bond length in the epoxide, both Mg^{2+} and H_3O^+ activators give the same bond lengths (1.55 Å), while Li^+ gives a shorter value (1.49 Å), revealing a somewhat weaker activation of the epoxide ring.

In the case of butene and cyclopentene oxides (Fig. 3), the steric effect of the substituents leads to DMSO/epoxide distances larger than those found with DMSO/ethylene epoxide (2.83 Å and 2.77 Å respectively vs 2.51 Å). All these structures lead to a transition state where the epoxide ring is opened and a bond is formed between the oxygen atom of the DMSO and the attacked carbon atom of the epoxide (see Fig. 3).

The largest structural evolutions starting from the CPX1 complex to the transition structures occurs in the case of activation by the Li^+ cation. Indeed, the C–O bond in TS1 is 1.88 Å, i.e. 0.39 Å longer than in the corresponding complex, and the C–O bond to be formed with DMSO has a length of 2.03 Å, *i.e.* 0.64 Å shorter than in CPX1. A contrario, the weakest evolutions are noted for the Mg^{2+} catalyst where the epoxide ring C–O bond only increases by 0.08 Å and the DMSO–epoxide distance decreases by 0.36 Å. In the case of H_3O^+, the evolution of the C–O bond to be formed is in the range 0.20 to 0.26 Å. The major difference in this series is reported for the C–O bond to be formed with DMSO—while this distance only decreases by 0.33 Å for the ethylene oxide, this contraction reaches ~0.50 Å for the CH_3– and –$(CH_2)_3$– substituted cases. This can be easily explained by the fact that this approach requires the reorganisation of the attacked carbon atom and of the substituent R, more difficult when R = CH_3– or –$(CH_2)_3$–.

In the α-hydroxyalkoxysulfonium products (PD1) the epoxide ring is clearly opened and the DMSO oxygen atom is bonded to the carbon atom of the epoxide (dC–O≈1.5–1.6 Å). Note however that the shortest distance is found for the Mg^{2+} case while, in contrast, the distance is the longest in TS1. The products obtained by the Lewis acids activation are made up of a single entity, since a tight bond is observed between the opened epoxide and the metal (d(O–A) = 1.64 Å and 1.77 Å for A = Li^+ and Mg^{2+}, respectively).

Energetics

In all cases, the transition states appear early in the reaction, as the distance between the oxygen atom of

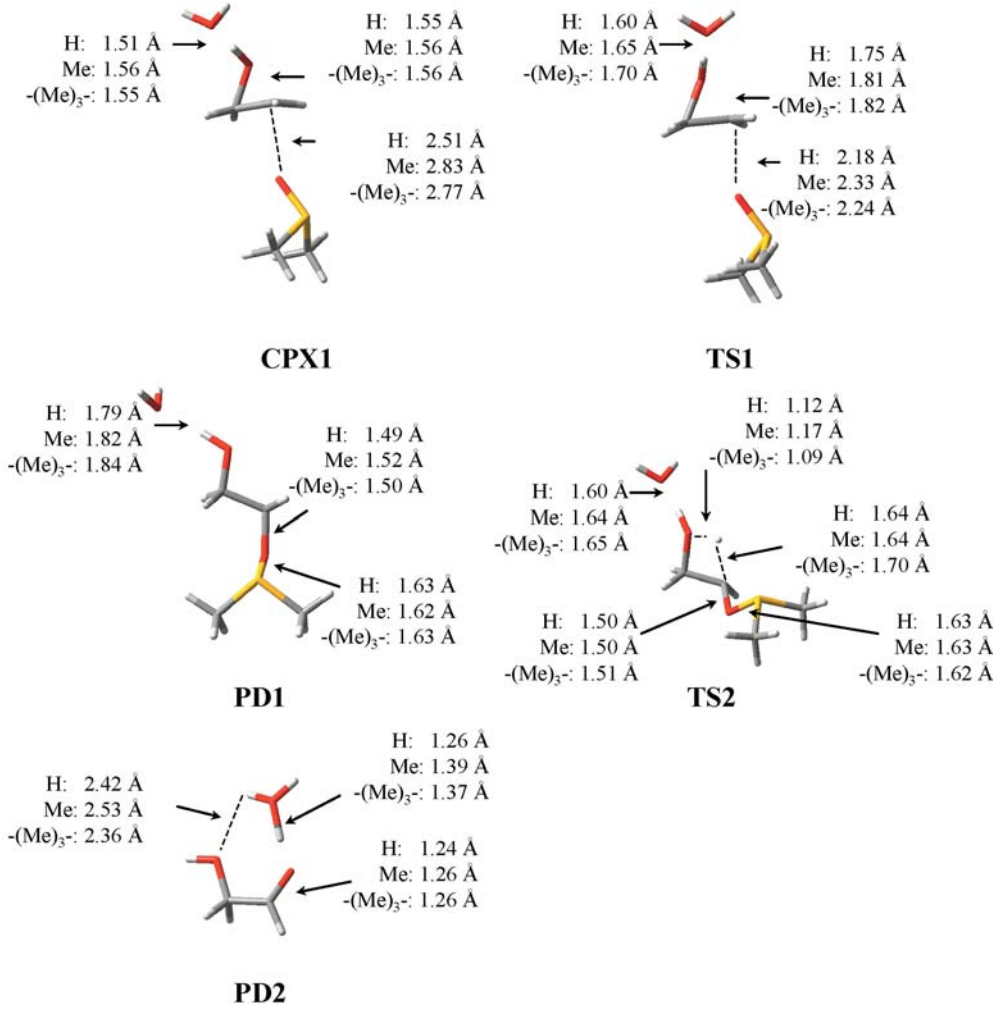

Fig. 3. Optimised structures with characteristic distances of the DMSO/substituted epoxide/H_3O^+ system. PD2 DMS molecule is not shown

DMSO and the epoxide carbon atom is smaller between the reactants and the TS than between the TS and the products. This early transition state leads to an exothermic reaction, according to Hammond's postulate. The energetics for the oxidative ring-openings initiated by various catalysts are summarised in Table 2.

The complex obtained between the activated epoxide and the DMSO solvent molecule requires an activation energy of less than 4 kcal·mol^{-1} for all the systems except **1**/Li^+, where this activation is 12.4 kcal·mol^{-1}. This result is in accordance with the weakest activation of the epoxide ring C–O bond noticed previously. However, it is clear that this low activation energy is easily overcome at room temperature, due to the well-known opening ability of epoxide ring [24], and is not the kinetically determining step.

The first step of the ring-opening is found to be exothermic in all cases, especially in the case of activation by Mg^{2+} where the exothermicity is evaluated to be 42.2 kcal·mol^{-1}.

Concerning the role of the substituents, note that *cis*- and *trans*-butene oxides lead to a weaker activation barrier than for the non-substituted epoxide and cannot be considered then to be large enough to perturb the approach of the DMSO towards the epoxide ring (see Fig. 3). Conversely, cyclopentene oxide presents an activation barrier that, although weak, is about three-fold larger than for ethylene oxide (4.2 kcal·mol^{-1}). For these products we observe weaker exothermicity than for ethylene oxide. The production of the alkoxysulfonium ion requires the rotation of the S–O bond of DMSO around the carbon atom of the epoxide. This rotation is more difficult in the case of substituted epoxide. This results in products more than 5 kcal·mol^{-1} higher in energy relative to the corresponding reactants than in the ethylene oxide case.

Table 2. Calculated Gibbs Free energies barriers ($\Delta G^{298\ K}$) of the stationary points on the potential energy surface at the B3LYP/6–31++G(d,p) level of theory, related to the starting complexes. See text for details

System/catalyst	CPX1	TS1	PD1	TS2	PD2
1/Li^+	0.0	12.4	−1.6	40.3	−56.1
1/Mg^{2+}	0.0	0.1	−42.1	2.7	−51.7
1/H_3O^+	0.0	1.5	−23.2	28.3	−41.6
$\mathbf{2}^{cis}$/H_3O^+	0.0	0.1	−17.7	36.7	−47.4
$\mathbf{2}^{trans}$/H_3O^+	0.0	1.3	−15.1	37.3	−46.8
3/H_3O^+	0.0	4.2	−16.9	38.5	−46.8

Atom charge distribution and polarisation energies

Atom charges have been obtained by the natural population analysis tool implemented in the Gaussian98 package. The polarisation of the O–M bond increases along the ring-opening reaction path. The largest effect is observed with the presence of the Mg^{2+} ion, where the epoxide oxygen atom charge decreases from −0.91e to −1.20e during the first step. Nevertheless, it has to be noted that in the meantime the charge of the Mg^{2+} cation increases drastically in the direction 1.64e, 1.88e, and 1.92e for CPX1, TS1, and PD1, respectively.

Concerning Li^+, its effect on the oxygen atom is comparable with that of Mg^{2+}, with evolution of the oxygen atom charge of ∼0.3e, but starting from a less polarised oxygen charge (−0.79e to −1.10e). The Li^+ charge remains very close to unity along the reaction path: 0.99e, 0.98e, and 0.97e for CPX1, TS1, and PD1, respectively. This may be partly rationalised by the hard acid [25] characteristic of this Lewis acid and led us to propose an analysis of the polarisation energy for such a complex. The polarisation component of the binding energy between Li^+ and the epoxide has been evaluated according to Eq. (1) at the B3LYP/6–31 + + G** level of theory. Energy discrimination between electrostatic and pure polarisation components can reasonably be performed when alkali cations are involved, due to small charge transfer [26]. The polarisation component of the epoxide/DMSO complex with Li^+ has been evaluated to be −29.9 kcal mol^{-1} which quantifies the large polarisability of such a compound. The total electrostatic component (polarisation and coulomb components) is found to be $-75.4\ kcal \cdot mol^{-1}$. Unfortunately, such analysis cannot reasonably be performed either with the Mg^{2+} Lewis acid, due to a too large charge transfer, or with the H_3O^+ catalyst, for which a hydrogen atom is transferred to the epoxide.

Concerning the charges in the H_3O^+-catalysed system, the proton remains strongly charged (evolution from 0.56e in CPX1, to 0.55e and 0.53e in TS1 and PD1, respectively), the ring oxygen atom charge thus decreases less in the three stationary points (evolution from −0.59e to −0.79e). Whichever the catalyst is, it produces a weak effect on the DMSO molecule. In all three cases ($A = H_3O^+$, Li^+, or Mg^{2+}), the DMSO oxygen atom charge decreases along the reaction path, due to the formation of a covalent bond with the epoxide carbon atom, although the sulfur atom keeps a large positive charge.

Conclusion

The analysis of the distance evolution, together with the charge distribution descriptions, leads us to a better understanding of the important energy difference between the Li^+ case and the other cases. It appears clearly that Li^+ shows a weaker polarisation strength than H_3O^+ or Mg^{2+} and leads a lower activation barrier for this first step. On the other hand, H_3O^+ and Mg^{2+} catalysts exhibit amazingly comparable effects although the means of lowering the barrier are completely different: important charge-transfer and polarisation effect in the Mg^{2+} case, as opposed to the creation of a covalent OH bond in the H_3O^+ case.

Carbon atom oxidation

This second step of the reaction is the oxidative process after the ring-opening step. From an experimental point of view, this step always requires strong activation, since it was reported to need basic treatment, high temperature [10], or microwave irradiation [27].

It has been checked that the starting structure for this step is PD1 since no structural reorganisation is necessary to directly reach TS2. The oxidation of the carbon atom is accomplished by elimination of a hydrogen atom and its transfer to the epoxide oxygen atom as a proton, which leads to the formation of an α-hydroxycarbonyl compound with regeneration of the activator and the production of dimethylsulfide (DMS) (see Scheme 1).

A reaction path which involves oxidation of the carbon atom through the transfer of the hydrogen atom to the DMS and formation of protonated DMS has been calculated to require an energy of $\sim 75\ kcal \cdot mol^{-1}$ in all the cases studied here. Such a reaction can thus be considered as marginal in the oxidative process and will not be described further.

Structural evolution

The transition state for this step, denoted TS2, features intramolecular proton transfer from the attacked carbon atom by DMSO towards the oxygen atom of the epoxide, accompanied by an elongation of the catalyst–oxygen atom distance.

Let us first consider ethylene oxide under the activating action of the three acids. Inspection of the structures (see Figs. 2 and 3) shows that the intramolecular proton transfer from the attacked carbon by DMSO to the vicinal oxygen atom is asymmetric. Indeed, in all the cases this proton is closer to the oxygen atom than to the carbon one. A slight difference exists between the H_3O^+ catalyst on one hand and the two Lewis acids on the other hand as this transfer is clearer in the former case ($dO...H^{transferred}$: 1.12 Å vs 1.18 Å and $C–H^{transferred}$: 1.64 Å vs 1.51–1.54 Å). On the DMSO side, both H_3O^+ and Li^+ activators lead to comparable results but Mg^{2+} case exhibits the shortest C–O distance and the longest S–O bond length.

Concomitant with these atom displacements, one has to consider also the elongation of the oxygen/activator bond which is part of the normal mode of the transition state. Here again, some discrepancies can be put forward between the two Lewis acid cases and the H_3O^+ one. In the metal activators cases, both the $O–Li^+$ and $O–Mg^{2+}$ distances increase (by 0.09 Å and 0.16 Å respectively).

For H_3O^+, the behaviour is completely different—the proton already covalently bonded to the oxygen atom is back-transferred to the water molecule. This leads to a decrease of the distance between the complex and the water molecule by 0.19 Å.

The effect of substitution is rather weak since the geometries obtained show structural parameters with values close to the ethylene/H_3O^+ system, except for one point concerning cyclopentene oxide. Indeed, in the corresponding transition state the hydrogen transfer is the most advanced among all the series we consider (dO–H: 1.09 Å and dC–O: 1.70 Å).

This hydrogen transfer along with elongation of the S–O distance leads, in all cases, to the products denoted PD2, which is composed of two sub-units, namely an α-hydroxycarbonyl compound bonded to the catalyst and a DMS molecule.

Atomic charges distribution

In TS2, the net atomic charges of the two metal cations are 0.98e and 1.41e for Li^+ and Mg^{2+} respectively, showing an important evolution of the charge transfer between the Mg^{2+} and the oxygen atom from PD1 to TS2. Concerning H_3O^+ activation the charge of the hydrogen atom bonded to the oxygen of the starting epoxide changes only slightly with respect to PD1 structure (0.56e in the present TS) indicating that it is still tightly bonded to the oxygen atom. The hydrogen atom being transferred and the corresponding oxygen atom show quite polarised charges. For Li^+ one obtains O: −1.05e and H: 0.41e; for Mg^{2+}, O: −1.02e and H: 0.44e; for H_3O^+, O: −0.79e and H: 0.46e.

The effect of the substitution is rather weak and leads to values comparable to the case of the H_3O^+/ethylene oxide molecular system.

Energetics

Values are listed in Table 2 and also indicated in Figs. 2 and 3. The ranking of the barrier heights has changed compared with the first step. In the second step the Li^+ system now leads to the weakest energy barrier of the series (+41.9 kcal mol^{-1}) while activation energies for Mg^{2+} and H_3O^+ are higher (+44.8 kcal·mol^{-1} and +51.5 kcal·mol^{-1}, respectively). This can be rationalised by the fact that no important charge transfer occurs between the Li^+ cation and the rest of the molecular system. Thus, the creation of the O–H bond leads only to an increase of the cation–oxygen atom distance. On the other hand, the same displacement for Mg^{2+} is more difficult, due to its double positive charge and to the important charge transfer which exists in the transition state structure. The higher barrier is found in the case of the H_3O^+ system where breaking of a covalent O–H bond has to be overcome to regenerate H_3O^+. This barrier is only slightly increased by substitution of ethylene oxide by butene or cyclopentene oxide. This increase is due to a spatial rearrangement of DMSO around the epoxide-attacked carbon which rotates around the C–C bond to present the hydrogen atom in a proper way to be transferred.

At this point, it has to be noted that the Mg^{2+} case is unique in the sense that the first step is much more exothermic than the other cases and that, in the following, the absolute energy of TS2 is about the energy of the starting complex (see Table 2). Nevertheless, all the activators lead to products stabilised by approximately the same amount of energy with respect to the starting complexes. Indeed going from TS2 to the products of the reaction, energies decrease in an important manner.

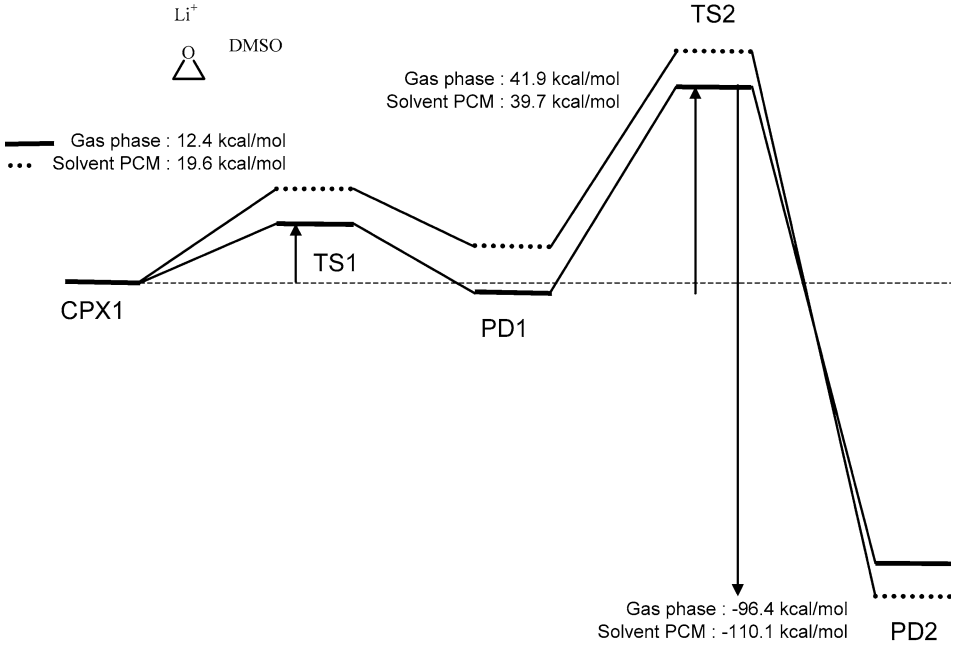

Fig. 4. Comparison between the reaction pathways in the gas phase and in DMSO for the Li^+-catalysed oxidative ring-opening of ethylene oxide

Solvation effects

Calculations have been carried out on the gas phase stationary points of the **1**/Li^+ system, considering the polarised continuum model of Tomasi and coworkers [28] for solvation by DMSO ($\epsilon = 46.7$). Corrections between electronic energy and free energy were taken from gas-phase values. Such calculations can provide a better understanding of the experimental reactions between the epoxide and Lewis or Brönsted acids in DMSO. Note that these points cannot be considered as stationary points in the B3LYP/PCM calculations and the corresponding energy values have to be analysed on a semiquantitative basis. The comparisons between the two reaction pathways are shown in Fig. 4.

From a qualitative point of view the results remain essentially the same with the higher activation barrier being found for the second step, *i.e.* the oxidation process. From a quantitative point of view, the large charge separation, which results in large dipole moments, leads to somewhat different energy values.

Considering the first step, we notice that the solvation effect destabilises PD1, making the first step endothermic (PD1 is 7.2 $kcal \cdot mol^{-1}$ higher in energy than CPX1). The second step of the process requires a lower energy than in the gas phase. Indeed, the large charge separation in TS2 is probably stabilised by the solvent electric field. The second step is then largely exothermic with stabilisation of more than 110 $kcal \cdot mol^{-1}$ in comparison with TS2.

Conclusion

We have conducted the first theoretical study on the mechanism of epoxide oxidative ring-opening by DMSO. Calculations have been performed with ethylene oxide, butene oxide, and cyclopentene oxide as the reactants and with H_3O^+ as the catalyst. Furthermore, two additional catalysts, namely Li^+ and Mg^{2+}, have been investigated with ethylene oxide as the reagent. We have described the two steps involved in such a reaction and compared the influence of the substituents and catalysts on the reaction free energies and activation barriers. We have shown that the substituents on ethylene oxide do not change considerably either qualitatively or quantitatively the energetics of the reactions. As for the role of the catalyst, Li^+ leads to the weakest oxidative process activation energy among the three catalysts. Also, we have shown that monovalent Lewis acid Li^+ and Brönsted acid H_3O^+ lead, from a qualitative point of view, to the same trends concerning the energy, but with different barrier heights for the Li^+ cation. The high oxidative step energy barrier is attributed to the difficult transfer of the intramolecular hydrogen atom, because of the need to overcome the positive electrostatic field created by the catalyst in the region of the oxygen atom of the epoxide.

Acknowledgements. J. Golebiowski and S. Antonczak seize the opportunity of this special issue to gratefully thank Pr. Jean-Louis Rivail for the great years spent in his laboratory.

References

1. March J (1992) Advanced organic chemistry, 4th edn. Wiley–Interscience, New York
2. Hodgson DM, Gras E (2002) Synthesis 12: 1625
3. Katsuki T, Sharpless BK (1980) J Am Chem Soc 102: 5974
4. Zhang W, Loebach JL, Wilson SR, Jacobsen EN (1990) J Am Chem Soc 112: 2801
5. Bonini C, Righi G (2002) Tetrahedron 58: 4981
6. Jacobsen EN, Wu MH (1999) Comprehensive asymmetric catalysis I–III. Springer, Berlin Heidelberg New York
7. Jacobsen EN (2000) Acc Chem Res 33: 421
8. Cohen T, Tsuji T (1961) J Org Chem 26: 1681
9. Gala D, DiBenedetto DJ (1994) Tetrahedron Lett 35: 8299
10. Santosusso TM, Swern D (1975) J Org Chem 40: 2764
11. Tsuji T (1989) Bull Chem Soc Jpn 62: 645–647
12. Inoue J, Nakamura M, Cui Y-S, Sakai Y, Sakai O, Hill JR, Wang KW, Yuen P-W (2003) J Med Chem 46: 868
13. Inagaki M, Matsumoto S, Tsuri T (2003) J Org Chem 68: 1128
14. Crich D, Neelamkavil S (2002) Tetrahedron 58: 3865
15. Coin C, Le boisselier V, Favier I, Postel M, Duñach E (2001) Eur J Org Chem 4: 735
16. Antoniotti S, Duñach E (2001) Chem Commun 2566
17. Antoniotti S, Duñach E (2004) J Mol Catal A 1/2: 135
18. Frisch MJ, Trucks GW, Schlegel HB, Scuseria GE, Robb MA, Cheeseman JR, Zakrzewski VG, Montgomery JA, Stratmann RE, Burant JC, Dapprich S, Millam JM, Daniles AD, Kudin KN, Strain MC, Farkas O, Tomasi J, Barone V, Cossi M, Cammi R, Mennucci B, Pomelli C, Adamo C, Clifford S, Ochterski J, Petersson GA, Ayala PY, Cui Q, Morokuma K, Malick DK, Rabuck AD, Raghavachari K, Foresman JB, Cioslowski J, Ortiz JV, Stefanov BB, Liu G, Liashenko A, Piskorz P, Komaromi I, Gomperts R, Martin RL, Fox DJ, Keith T, Al-Laham MA, Peng CY, Nanayakkara A, Gonzalez C, Challacombe M, Gill PMW, Johnson BG, Chen W, Wong MW, Andres JL, Head-Gordon M, Replogle ES, Pople JA (1998) Gaussian 98, Revision E7 edn. Gaussian, Pittsburg, PA
19. Becke AD (1993) J Chem Phys 98: 5648
20. Lee C, Yang W, Parr RG (1988) Phys Rev B 37: 785
21. Cubbage JW, Guo Y, McCulla RD, Jenks WS (2001) J Org Chem 66: 8722
22. Turecek F (1998) J Phys Chem 102: 4703–4713
23. Laitinen T, Rouvinen J, Peräkyla M (1998) J Org Chem 63: 8157
24. Banks HD (2003) J Org Chem 68: 2639
25. Pearson RG (1968) J Chem Educ 45: 581–587
26. Golebiowski J, Lamare V, Ruiz-Lopez MF (2002) J Comput Chem 23: 724
27. Villemin D, Hammadi M, (1995) Synth Commun 25: 3141
28. Tomasi J, Persico M (1994) Chem Rev 94: 2027